Magnetodielectric and magnetoviscosity response of a ferromagnetic liquid crystal at low magnetic fields

Rasmita Sahoo, M. V. Rasna, D. Lisjak, A. Mertelj, and Surajit Dhara

Citation: Applied Physics Letters **106**, 161905 (2015); doi: 10.1063/1.4918995
View online: http://dx.doi.org/10.1063/1.4918995
View Table of Contents: http://scitation.aip.org/content/aip/journal/apl/106/16?ver=pdfcov
Published by the AIP Publishing

Magnetodielectric and magnetoviscosity response of a ferromagnetic liquid crystal at low magnetic fields

Rasmita Sahoo,[1] M. V. Rasna,[1] D. Lisjak,[2] A. Mertelj,[2] and Surajit Dhara[1,a)]
[1]*School of Physics, University of Hyderabad, Hyderabad 500046, India*
[2]*J. Stefan Institute, Jamova cesta 39, Ljubljana SI-1001, Slovenia*

(Received 21 January 2015; accepted 13 April 2015; published online 23 April 2015)

We report on experimental studies of the viscoelastic, magnetodielectric, and magnetoviscosity properties of ferromagnetic liquid crystals (LCs) prepared by dispersing ferromagnetic nanoparticles in a thermotropic LC. Both the splay elastic constant and rotational viscosity of the ferronematic LCs are found to be considerably lower than that of the pure LC and advantageous to the device applications. The ferromagnetic LCs show unique magnetodielectric and magnetoviscosity response at very low magnetic fields that are useful for smart fluid applications. © *2015 AIP Publishing LLC*. [http://dx.doi.org/10.1063/1.4918995]

Ferrofluids are liquids prepared by suspending nanometer-sized ferromagnetic particles in isotropic carrier fluids. The magnetic attraction of nanoparticles is weak enough that the entropic forces of the particles and steric and/or electrostatic repulsion due to the surfactant prevents magnetic clumping or agglomeration. The magnetic moments of the nanomagnets are aligned along the direction of the external magnetic field resulting in chain formation due to the dipole-dipole interaction. As a result, the viscosity of the ferrofluids increases significantly and these materials are useful for various magnetorheological applications.[1–3] Long ago, Brochard and de Gennes theoretically predicted various interesting properties of *anisotropic* ferrofluids that can be prepared by dispersing different types of ferromagnetic nanoparticles in nematic liquid crystals (NLCs). They provided a continuum theory of magnetic suspensions in NLCs and so contrived the term as ferronematics.[4] In spite of several attempts in the past, only very recently the successful experimental realization of a ferromagnetic liquid crystalline material was reported by Mertelj *et al.*[5] They prepared colloidal suspension of platelet type ferromagnetic nanoparticles in pentyl cyanobiphenyl (5CB) liquid crystal at room temperature. Subsequently, they reported on magnetooptic and converse magnetoelectric effects in these materials and described the system by a simple macroscopic theory.[6]

Nematic liquid crystals exhibit anisotropic physical properties. The colloidal dispersion of nanoparticles (with low concentration) in liquid crystals does not affect the overall molecular orientation. Nevertheless, the small particles affect significantly the anisotropic physical properties that depend on the size, shape, concentration, and properties of the nanoparticles.[7–18] The colloidal dispersion of nanoparticles in liquid crystals combines the physical properties of nanoparticles and the orientational order of liquid crystals. There are a few reports on the physical measurements of liquid crystal nanocomposites based on ferromagnetic nanoparticles. The experimental results showed that the nanocomposites are paramagnetic.[18,19] The recent discovery of unambiguous ferromagnetic liquid crystals by Mertelj *et al.*[5] has created immense interest in the scientific community. A suspension of ferromagnetic nanoplatelets in a NLC can be macroscopically described by coupled $\vec{M}$ and $\hat{n}$, where $\vec{M}$ describes the density of magnetic moments. The coupling is a result of the interaction of the NLC with the surface of the nanoplatelets. $\vec{M}$ directly responds to magnetic and $\hat{n}$ to electric fields. However, due to their coupling, $\vec{M}$ also indirectly responds to electric field and inversely $\hat{n}$ to small magnetic fields. In this letter, we report on the measurements of splay elastic constant, rotational viscosity, magnetodielectric, and the magnetoviscosity response of ferromagnetic LCs. We show that the viscoelastic properties are considerably lower than the pure sample and unique magnetodielectric and magnetoviscosity response at very low magnetic fields.

We used 4-cyano-4′-octylbiphenyl (8CB) liquid crystal obtained from Sigma-Aldrich. It exhibits the following phase transitions: I 38.8 °C N 32.5 °C SmA 21.5 °C Cr. We prepared isotropic suspension of scandium-doped barium hexaferrite single-crystal ($BaFe_{11.5}Sc_{0.5}O_{19}$) magnetic nanoplatelets in isopropanol. The thickness of the platelets is about 5 nm, the distribution of the platelet diameter is approximately 70 nm, and the standard deviation is 38 nm. The details of the preparation of the magnetic nanoplatelets and preliminary characterization are reported in Ref. 20. The preparation of ferronematic sample and the experimental techniques are briefly mentioned in the supplementary material.[21]

Figure 1(a) shows the TEM image of the nanoplatelets. Figure 1(b) shows the physical appearance of the suspensions in the nematic phase. The sample appears reddish with increasing concentration of the nanoparticles. Figures 1(c) and 1(d) show the photomicrographs of a planar cell obtained from polarising optical microscope. The director (the average alignment direction of the LC molecules) is aligned uniformly along the rubbing direction with no evidence of large agglomeration of the platelets. A schematic orientation of the magnetic nanoplatelets together with the LC director and cross-section of disclination lines is also shown in Fig. 1(e). The direction of magnetization is perpendicular to the plane of the nanoplatelets. The LC director is anchored perpendicular to the nanoparticle's surface and

a)Electronic mail: sdsp@uohyd.ernet.in

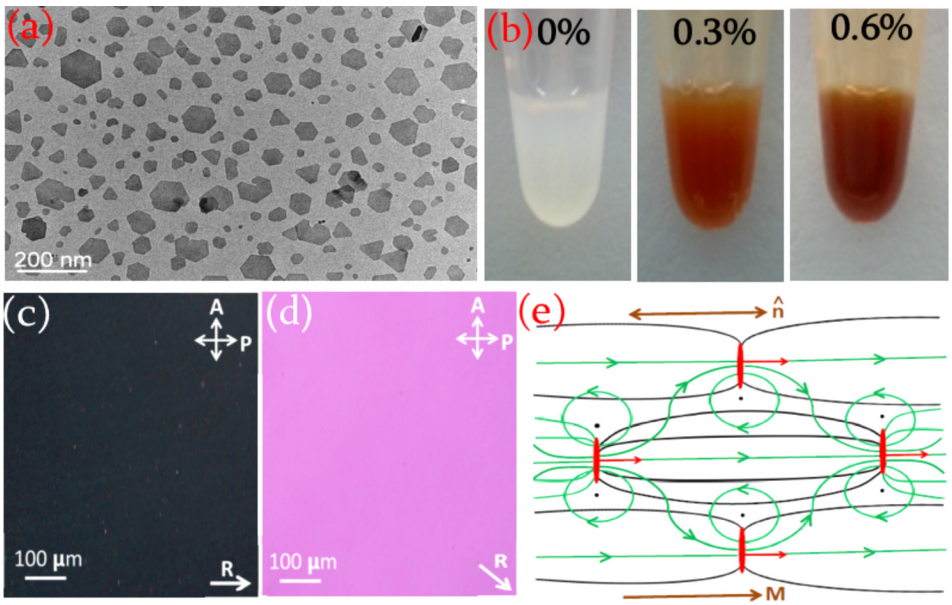

FIG. 1. (a) TEM image of the nanoplatelets. (b) Magnetic nanoplatelets suspended in 8CB liquid crystal at three different concentrations: 0 wt. %, 0.3 wt. %, and 0.6 wt. % at 35 °C. (c) Photomicrographs of aligned cell of a ferromagnetic suspension (0.6 wt. % magnetic nanoplatelets) under optical polarized microscope, polariser (P) and analyser (A) are crossed and the rubbing direction (R) parallel to P (d) the rubbing direction is at 45° with respect to P and A. (e) A schematic presentation of the director, $\hat{n}$ (black) and the magnetic field (green) around the platelets (red and vertical short-lines). Black dots represent cross-section of disinclination lines. Photomicrographs (c) and (d) are taken in the absence of magnetic field.

forms a stable suspension with a macroscopic magnetization along the director.[5]

First, we present and discuss some physical properties measured in the absence of magnetic field. Figure 2(a) shows the temperature dependence of parallel ($\epsilon_{||}$) and perpendicular ($\epsilon_{\perp}$) components of dielectric constant. It is observed that the dielectric anisotropy $\Delta\epsilon$ ($= \epsilon_{||} - \epsilon_{\perp}$) remains unaffected by the incorporation of nanoparticles. For example, in all the samples, $\Delta\epsilon \simeq 8$. The dielectric anisotropy is proportional to the scalar order parameter S of a nematic LC.[22] This result suggests that the magnetic nanoparticles do not disturb nematic order significantly. Figure 2(b) shows the temperature dependence of splay elastic constant (K_{11}). K_{11} was measured directly from the Frederiks threshold voltage,[22] i.e., $V_{th} = \sqrt{K_{11}/\epsilon_o \Delta\epsilon}$, ϵ_o being the permittivity of the free space. It is observed that K_{11} decreases (Fig. 2(b)) with increasing concentration of magnetic nanoparticles. For example, at a particular temperature (35 °C), K_{11} in the suspension (with 0.6 wt. % magnetic nanoparticles) decreases by 22% compared to the pure LC. The rotational viscosity (γ_1) was measured from the measurement of relaxation time (τ_o) in a planar cell using a phase-decay-time measurement technique[23,24] (see supplementary material). The temperature variation of γ_1 is shown in Fig. 2(c). It is observed that γ_1 decreases with increasing concentration of magnetic nanoparticles. For example, at 35 °C, γ_1 (0.6 wt. % nanoparticles) is reduced by 11% compared to the pure nematic LC. In the mean field theory,[22,25] both $K_{11} \propto S^2$ and $\gamma_1 \propto S^2$. The decrease of S in the suspensions (0.6 wt. % magnetic nanoparticles), according to dielectric anisotropy measurement is less than 4%. Hence, the decrease of K_{11} and γ_1 cannot be due to the decrease of S alone as both decrease more than that expected from the decrease of S.

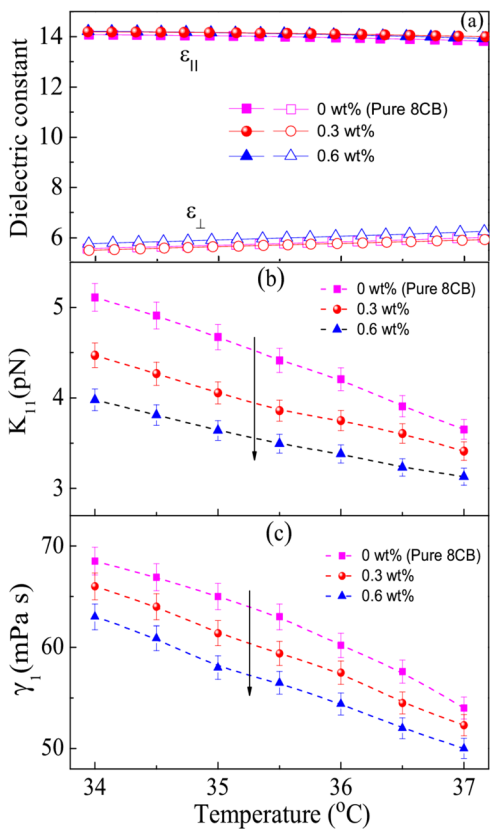

FIG. 2. Temperature variation of (a) parallel ($\epsilon_{||}$) and perpendicular ($\epsilon_{\perp}$) components of dielectric constant, (b) splay elastic constant (K_{11}), and (c) rotational viscosity (γ_1) in the nematic phase. Vertically downward arrows indicate the decrease of respective properties with increasing concentration of magnetic nanoparticles. Cell thickness 13.1 μm.

To study the magnetodielectric effect, the sample was filled in a planar cell and the magnetic field was applied perpendicular to the director ($\hat{n}$), i.e., $\vec{B} \perp \hat{n}$. Figure 3(a) shows the variation of effective dielectric constant (ϵ_{eff}) with magnetic field in pure 8CB. ϵ_{eff} increases rapidly beyond the Frederiks threshold magnetic field ($\simeq$128 mT) (Fig. 3(a)) and tend to saturate at higher field as expected. The magnetic field dependence of ϵ_{eff} in the suspensions is significantly different. The cells were filled in the absence of external magnetic field, so initially they were magnetically polydomain state. During the first measurement (Fig. 3(b)), we observed that ϵ_{eff} increases slightly with magnetic field up to 4 mT, and beyond this field it increases steeply. Finally, it saturates above the magnetic field of 10 mT. The saturation

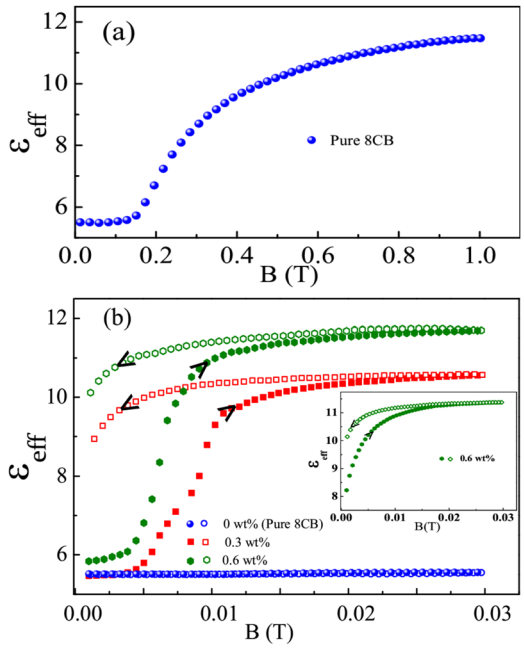

FIG. 3. (a) Variation of effective dielectric constant (ϵ_{eff}) with magnetic field (B) of pure 8CB at 36 °C. (b) Variation of ϵ_{eff} with magnetic field of a few samples with different concentrations: 0 wt. % (blue spheres), 0.3 wt. % (red squares), and 0.6 wt. % (green hexagons). Upward and downward arrows indicate the data collected during increasing and decreasing of the magnetic field. (Inset) Magnetodielectric response from the same sample in the second measurement. Cell thickness of 58 μm. Applied voltage of 0.6 V and frequency of 3.111 kHz.

in ϵ_{eff} is a signature of a magnetically monodomain state. In the decreasing field, it shows hysteresis in the dielectric constant. It is due to the transformation from a polydomain to a monodomain state. However, due to the domain wall pinning at the surface imperfections, this transformation is not complete; as a result, we also observe the hysteresis in the successive measurements. The second measurement was performed 20 min after the first one. During this time, the value of ϵ_{eff} (at 1 mT) is reduced from 10 to 8, which shows that the additional magnetic relaxation of the sample occurred (e.g., slow motion of domain walls). In the second measurement, ϵ_{eff} steeply increases with the external field as expected in a monodomain sample (inset of Fig. 3(b)). In the decreasing field, the curve is almost identical to the first measurement. The time lapse between two successive measuring points in both measurements was 30 s. The first measurement thus shows the growth of magnetic domains, which is governed by the motion of domain walls and during this measurement the sample is almost transformed from polydomain to a monodomain state. In pure 8CB, $\hat{n}$ is directly coupled to $\vec{B}$, whereas in the suspensions the coupling between $\hat{n}$ and $\vec{B}$ is indirect. The external magnetic field $\vec{B}$ directly induces reorientation of magnetization $\vec{M}$ and since $\vec{M}$ is coupled to the orientation of $\hat{n}$, $\vec{B}$ indirectly causes a reorientation of $\hat{n}$. The latter results in the increase of ϵ_{eff}. As explained in Ref. 6, the reorientation of $\hat{n}$ is smaller than the reorientation of $\vec{M}$ and so the saturated value of ϵ_{eff} in the suspensions is smaller (Fig. 3(b)) than in the pure 8CB (where orientation of $\hat{n}$ is directly coupled with the external field) (Fig. 3(a)). We observe that the saturated value of ϵ_{eff} in the suspensions with higher concentration of platelets is larger (Fig. 3(b)). This is expected, since the saturated value depends on the coupling between $\vec{M}$ and $\hat{n}$, which is larger for higher density of the nanoplatelets.

Magnetoviscosity was measured by using a rheometer (Anton Paar MCR-501) with parallel plates having diameter of 20 mm (MRD-170) and plate-gap of 0.2 mm. The direction of the magnetic field is perpendicular to the plane of the plates. A schematic experimental setup of the magnetoviscosity measurement is shown in Fig. 4. Figure 5 shows the variation of shear viscosity with magnetic field. In pure 8CB, the shear viscosity (η_{eff}) at zero magnetic field is 25 mPa s and it is comparable to the Miesowicz viscosity η_2 of the nematic phase of the pure 8CB.[26] It suggests that the untreated plates of the rheometer induce almost planar alignment of the director along the shear direction (Fig. 4(b)). As the magnetic field is increased, the viscosity increases beyond 120 mT and reaches to about 40 mPa s around 1 T. The measured viscosity in the decreasing field is lower than that measured during increasing magnetic field. This is because in the freshly loaded samples usually there are many defects (disclination lines) and the sample is less homogeneous. In the ferromagnetic LC, the viscosity exhibits three distinct regimes. In the very low field region (below 10 mT), η_{eff} ($\simeq \eta_2$) is almost constant and increases rapidly in the intermediate field range (10 mT to 20 mT). At relatively higher field, η_{eff} saturates and exhibit hysteresis, while the field is reduced to zero (Fig. 5(b)). In the suspension with 0.3 wt. % magnetic nanoparticles, at zero

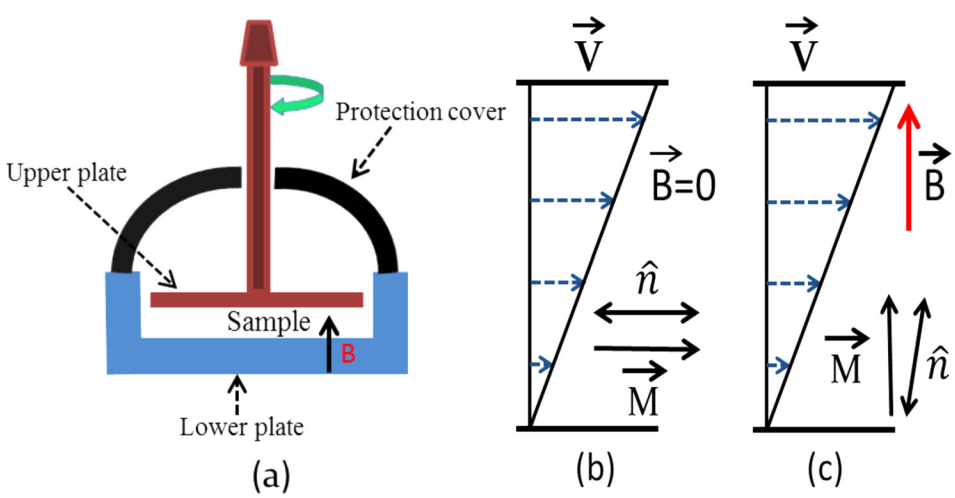

FIG. 4. (a) Schematic setup for the measurement of magnetoviscosity. The green arrow shows the direction of shear. The applied magnetic field (red arrow) is perpendicular to the shear direction. Orientation of director ($\hat{n}$) and magnetization ($\vec{M}$) at (b) zero and (c) finite field. The horizontal dotted lines represent the direction and magnitude of shear velocity ($\vec{V}$).

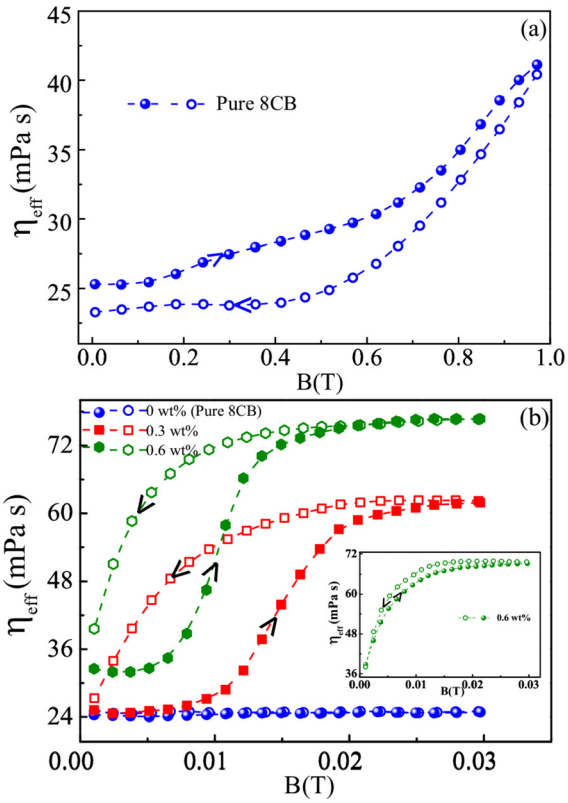

FIG. 5. (a) Variation of shear viscosity (η_{eff}) with magnetic field of pure 8CB LC and (b) suspensions with different concentrations: 0 wt. % (blue spheres), 0.3 wt. % (red squares), and 0.6 wt. % (green hexagons) at shear-rate of $10\,s^{-1}$. Upward and downward arrows indicate the data collected during increasing and decreasing of the magnetic field. (Inset) Magnetoviscosity response from the same sample (0.6 wt. %) in the second measurement. The measurements in the suspensions are restricted up to the field of 30 mT.

magnetic field, $\eta_{eff} = 25$ mPa s and it increases up to 62 mPa s in the saturation region and finally reduced to 27 mPa s at zero field. The viscosity at the zero field is equal to that of the pure 8CB sample and hence comparable to Miesowicz viscosity η_2. The effective viscosity in the saturated region is almost comparable to the Miesowicz viscosity η_1 of the pure 8CB at the same temperature.[26] This suggests that the director is almost parallel to the magnetic field (perpendicular to the shear direction) as schematically shown in Fig. 4(c). This technique thus helps us to measure two Miesowicz viscosities using a very small magnetic field. In the suspension with 0.6 wt. % magnetic nanoparticles, the overall behavior is almost similar except that the values are larger and this is expected as the viscosity is linearly proportional to the phase volume of the nanoparticles.

The magnetic field dependence of viscosity at the first measurement is significantly different from the second measurement and somewhat similar to that is observed in the magnetodielectric measurements. We attribute this behavior to the growth of magnetic domains, resulting in the magnetically monodomain sample as mentioned previously. The second measurement thus shows the behavior of a monodomain sample. In the second measurement at the smallest field (1 mT), the viscosity is larger than that is measured at the first measurement, further it steeply increases and saturates above $\simeq$15 mT (inset of Fig. 5(b)). In the magnetodielectric measurements, there is a competing orienting mechanism. The cell surfaces induce parallel orientation of the director, and the magnetic field induces perpendicular orientation of the same. On the other hand, in the rheological experiment, parallel orientation is induced by flow and this competes with the magnetic alignment (Figs. 4(b) and 4(c)).

In conclusion, we showed that the splay elastic constant and rotational viscosity are reduced in the ferronematic LC. The low field magnetodielectric and magnetoviscosity responses remarkably differ in the suspension from the pure LC due to the orientational coupling between the director field and the magnetization. The low magnetic field effects in these ferronematic materials make them useful for multipurpose applications because these are useful for both display and non-display applications such as a smart fluid. The small amount of magnetic nanoparticles (e.g., 0.3 wt. %) do not change the Miesowicz viscosities but facilitate the measurement at a significantly low magnetic field.

We gratefully acknowledge the support from the UPE-II, DST (SR/NM/NS-134/2010), CSIR (03(1207)/12/EMR-II), and DST-PURSE. M.V.R. and R.S. acknowledge UGC-BSR for fellowship. A.M. and D.L. acknowledge the support from Slovenian Research Agency (A.M., Grant No. P1-0192; D. L., Grant No. P2-0089-4).

[1]S. Odenbach and S. Thurm, *Magnetoviscous Effects in Ferrofluids* (Springer, Berlin, 2002).
[2]B. M. Berkovsky, V. F. Medvedev, and M. S. Krakov, *Magnetic Fluids: Engineering Applications* (Oxford University Press, Oxford, 1993).
[3]*Magnetic Fluids and Applications Handbook*, edited by B. Berkovski and V. Bashtovoy (Begell House, Wallingford, 1996).
[4]F. Brochard and P. G. de Gennes, J. Phys. France (Paris) **31**, 691 (1970).
[5]A. Mertelj, D. Lisjak, M. Drofenik, and M. Copic, Nature **504**, 237 (2013).
[6]A. Mertelj, N. Osterman, D. Lisjak, and M. Copic, Soft Matter **10**, 9065 (2014).
[7]M. Rahman and W. Lee, J. Phys. D: Appl. Phys. **42**, 063001 (2009).
[8]R. Basu and G. S. Iannacchione, Phys. Rev. E **81**, 051705 (2010).
[9]R. Basu and G. S. Iannacchione, Phys. Rev. E **80**, 010701(R) (2009).
[10]R. Manda, V. Dasari, P. Sathyanarayana, M. V. Rasna, P. Paik, and S. Dhara, Appl. Phys. Lett. **103**, 141910 (2013).
[11]M. V. Rasna, K. P. Zuhail, R. Manda, P. Paik, W. Haase, and S. Dhara, Phys. Rev. E **89**, 052503 (2014).
[12]J. F. Blach, S. Saitzek, C. Legrand, L. Dupont, J. F. Henninot, and M. Warenghem, J. Appl. Phys. **107**, 074102 (2010).
[13]M. Kaczmarek, O. Buchnev, and I. Nandhakumar, Appl. Phys. Lett. **92**, 103307 (2008).
[14]Y. Reznikov, O. Buchnev, O. Tereshchenko, V. Reshetnyak, A. Glushchenko, and J. West, Appl. Phys. Lett. **82**, 1917 (2003).
[15]L. Wang, W. He, X. Xiao, M. Wang, M. Wang, P. Yang, Z. Zhou, H. Yang, H. Yu, and Y. Lu, J. Mater. Chem. **22**, 19629 (2012).
[16]A. Glushchenko, C. I. Cheon, J. West, F. Li, E. Buyuktanir, Y. Reznikov, and A. Buchnev, Mol. Cryst. Liq. Cryst. **453**, 227 (2006).
[17]W. Jian, L. Yu, C. Yonglie, L. Zhaoxi, X. Ying, L. Ziyang, S. Longpei, and Z. Jianying, J. Mater. Sci. Mater. Electron. **12**, 597 (2001).
[18]P. Kopcansky, I. Potocova, M. Koneracka, M. Timko, A. G. M. Jansen, J. Jadzyn, and G. Czechowski, J. Magn. Magn. Mater. **289**, 101 (2005).
[19]N. Podoliak, O. Buchnev, O. Buluy, G. D'Alessandro, M. Kaczmarek, Y. Reznikov, and T. J. Sluckin, Soft Matter **7**, 4742 (2011).
[20]D. Lisjak and M. Drofenik, Cryst. Growth Des. **12**, 5174 (2012).
[21]See supplementary material at http://dx.doi.org/10.1063/1.4918995 for experimental details.
[22]P. G. de Gennes, *The Physics of Liquid Crystals* (Clarendon Press, Oxford, 1974).
[23]S. T. Wu and C. S. Wu, Phys. Rev. A **42**, 2219 (1990).
[24]P. Sathyanarayana, V. S. R. Jampani, M. Skarabot, I. Musevic, K. V. Le, H. Takezoe, and S. Dhara, Phys. Rev. E **85**, 011702 (2012).
[25]W. H. de Jeu, *Physical Properties of Liquid Crystalline Materials* (Gordon and Breach Science Publishers, New York, 1980).
[26]A. G. Chmielewski, Mol. Cryst. Liq. Cryst. **132**, 339 (1986).